

# The Subaperture Secondary Range Compression Algorithm for near space squint SAR

Yi Sun, Xiaojun Jing, Songlin Sun, Hai Huang

School of Information and Communications Engineer, Beijing University of Posts and Telecommunications

Key Laboratory of Trustworthy Distributed Computing and Service (BUPT), Ministry of Education, Beijing University of Posts and Telecommunications, Beijing, China  
sunyia999@163.com, jxiaojun@bupt.edu.cn, slsun@bupt.edu.cn, huanghai@bupt.edu.cn

**Abstract**—This paper discusses squint synthetic aperture radar (SAR) imaging in the near space platform and proposes an improved Secondary Range Compression (SRC) Algorithm, Subaperture Secondary Range Compression (SSRC) Algorithm. The key step is to use the subaperture approach in the SRC algorithm. First, the original signals are divided into subapertures in the azimuth direction of the time domain to image independently, and then the sub-bands of the frequency domain are combined to form the final SAR image. The method reduces coupling in the range and azimuth direction of the echo signal under the squint imaging mode, and addresses the problems of squint SAR in near space including overlong synthetic aperture and motion error. Simulation through point targets demonstrates the improvement in azimuth resolution, ISLR and PSLR, which verifies the effectiveness of this proposed SSRC algorithm in near space squint SAR imaging.

**Keywords**—Near space, squint SAR imaging, subaperture approach, Secondary Range Compression algorithm.

## I. INTRODUCTION

Near space refers to the airspace region from about 20 kilometer(km) to 100km above the earth's surface. Deployment of a platform in this region between satellites and low-altitude aircraft has unique advantages including good mobility survival ability, long hang time, wide covering scope and rapid reaction ability [1]. It has important significance and widely military application prospect on communication, detection, imaging and intelligence gathering. Near space SAR, as the

payload of a near space slow platform, has become an important supplement to satellite-borne SAR and airborne SAR, because of certain advantages. Its imaging area includes not only the area directly underneath the platform, but also a large squint area [2]-[3], which leads to a bigger squint angle than airborne SAR. Under the squint imaging mode, coupling will emerge in the range and azimuth direction of the echo signal, as well as range migration [4]. Conventional Range Doppler Algorithm (RDA) in side looking mode cannot satisfy the requirements of squint imaging [5]. The SRC algorithm, as an improvement over RDA, introduces a secondary range compression factor, relying on the Doppler centroid and Doppler rate to improve the focus performance in the range direction [6]. Range migration revision and direction processing is then done to improve the RDA imaging performance in squint situations.

Due to the slow motion and height characteristics of near space platforms, the near space SAR system achieves longer aperture time and aperture length than airborne SAR. At the same time, as with the squint angle increases, aperture length also substantially becomes longer, which leads to coupling and range migration between the range and azimuth directions[7]-[8]. This paper proposes an improved SRC algorithm based on subaperture approach, SSRC algorithm. This algorithm is applicable to the squint SAR imaging mode in near space. It reduces the serious coupling in the range and azimuth directions of the echo signal under

the squint imaging mode, and addresses the problems of squint SAR in near space including overlong synthetic aperture and motion error.

The structure of this paper is as follows. In Section II, the squint geometrical model of near space squint SAR is developed, then the SRC in squint SAR is discussed and the necessity of aperture division is presented. In Section III, the principle and process of SSRC algorithm are introduced in detail. In Section IV, simulation results and analysis which can verify this new algorithm to be more effective are presented. Finally, Section V includes conclusions.

## II. THE SQUINT GEOMETRICAL MODEL OF NEAR SPACE SAR

### A. Geometrical model

The squint geometrical model of near space SAR is shown in Fig.1. In order to facilitate discussion, we assume that the radar platform uniformly flies along the  $x$  axle ideally by the speed of  $v$  and keeps the height of  $H$  in a straight line. The incidence angle of the antenna beam view to the ground is  $\beta$ . Another hypothesis is that Point  $P_1$  is the center moment of slow time and antenna beam center line point to the center reference target point  $P$  of imaging scene at this moment. Point  $P_2$  is the radar location at the shortest squint distance  $R_0$ .  $\theta$  is the antenna squint angle. Assume that the time interval of  $P_1$  and  $P_2$  is  $t_m$ , then the distance between  $P_1$  and  $P_2$  is  $vt_m$ .

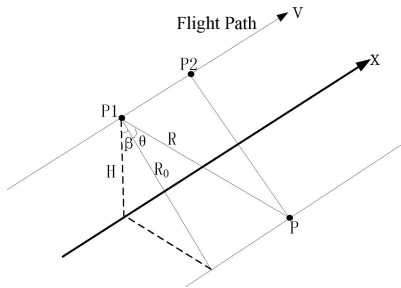


Fig.1. Squint geometrical model of near space SAR

The signal of squint SAR is a chirp signal. The echo signal of target point  $P$  can be described as

$$s(t, t_m) = \text{rect} \left[ \frac{t - 2R(t_m)/c}{T_p} \right] \text{rect} \left( \frac{t_m}{T_a} \right) \exp \left[ j\pi k_r \left( t - \frac{2R(t_m)}{c} \right)^2 \right] \exp \left[ -j4\pi \frac{R(t_m)}{\lambda} \right] \quad (1)$$

$$R(t_m) = \frac{H / \cos \beta}{\cos \theta} \quad (2)$$

Where  $T_p$  is the pulse width,  $T_a$  is the synthetic aperture length of target point  $P$ ,  $t$  is the range direction time,  $t_m$  is the azimuth direction time,  $R(t_m)$  is the instantaneous squint distance between radar and target point  $P$ ,  $k_r$  is the range direction rate.

### B. Discuss on SRC in squint SAR

Under low squint angle, the distance equation between radar and target point is approximated to the time parabola form. As the squint angle is increasing, the relationship between time and frequency is nonlinear, which will cause two effects: First, the range used in range migration revise and azimuth matched filter should adjust appropriately based on new range equation. Secondly, it will introduce coupling between the range and azimuth directions, and we should revise the defocus caused by coupling through filtering. This filtering method is called Secondary Range Compression [9].

### C. The necessity of aperture division

Considering the various aspects of the factors including the position of the platform, imaging mode and calculation efficiency, we discuss the necessity of aperture division for the near space squint SAR platform and then present the SSRC algorithm.

First, the subaperture algorithm is suitable for the special scene imaging given that the synthetic aperture time is quite long [10]. Due to the slow motion character and height character of the near

space platform, it has a longer aperture time and aperture length than airborne SAR. Therefore, it is necessary to divide into subapertures for the accurate high resolution imaging in near space SAR.

Secondly, the platform of near space SAR has a huge cover area. The imaging area not only includes the area directly underneath the platform, but also includes a large squint imaging area. The results of airborne SAR imaging vary greatly in the different squint angle. Furthermore, under the large-angle imaging scene, additional motion compensation mechanism is typically required, especially in the near space. Research shows that as the squint angle becomes bigger aperture length also substantially becomes longer. In order to realize the large area coverage, the big aperture needs to be divided into small subaperture to compensate, so as to ensure the quality of SAR image [11].

Thirdly, the subaperture processing will make the focusing, motion error estimation and compensation more accurate. In the full aperture there is only one reference position, and this will make more errors if synthetic aperture is very large. After dividing into subapertures, each aperture has its own reference center and reference distance, so the errors can be greatly decreased. In addition, each aperture can be processed in parallel [12].

For these reasons, subaperture processing is necessary for squint SAR imaging.

### III. THE SUBAPERTURE SECONDARY RANGE COMPRESSION (SSRC) ALGORITHM

Fig.2 shows the SSRC imaging process. First, the original data is divided into small subapertures. Then, imaging is performed in each subaperture independently. Finally, the sub-bands are combined to form the final SAR image.

#### A. Aperture division in azimuth

The amount of SAR image data in near space is enormous, and the calculation required is also

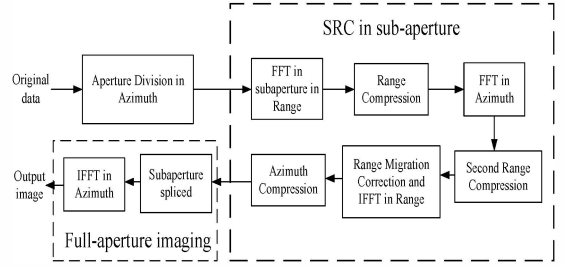


Fig.2. Flow chart of SSRC algorithm

quite large. The velocity is so slow that there exist some errors in synthetic aperture. We must divide them to some subapertures and then compensate respectively. In the azimuth direction, the method used is to divide the long aperture to different segments called subapertures and image each subaperture to form sub-images. Then superimpose these subimages to form the final fullaperture image.

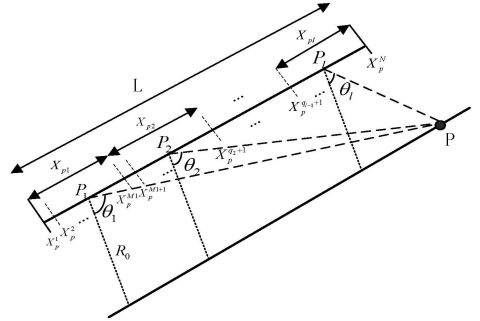


Fig.3. Geometric model of subaperture division

As is shown in Fig.3,  $x_p \in \{x_p^1, x_p^2, \dots, x_p^N\}$ , where  $x_p^k$  is the  $k$ -th azimuth,  $k=1, 2, \dots, N$ ,  $N$  is the total number of pulses in  $L$  aperture length. Next, divide the full aperture to some subapertures. Then  $x_p$  can be expressed as

$$x_p \in X_{p1} \cup X_{p2} \cup \dots \cup X_{pl}. \quad (3)$$

Where  $X_{pi} = \{x_p^{q_i+1}, \dots, x_p^{q_{i+1}}\}$ ,  $q_0 = 0$ ,  $q_i = \sum_{j=1}^i M_j$  refers to the  $i$ -th subaperture,  $l$  is the total number of

subapertures,  $M_i$  refers to the total number of pulses,  $x_p \in X_p$ ,  $i=1,2,\dots,l$ . Now the subaperture division has down. Typically in the theoretical analysis and simulation, the aperture can be equally divided.

For instance, the aperture length of the  $i$ -th subaperture can be considered as  $L_i = L/l$ ,  $P_i$  is the centre point of each subaperture, then each azimuth squint angle is

$$\theta_i = \arctan(\tan \theta + (2i-l-1) \cdot \frac{L_i}{2R_0}), i=1,2,\dots,l. \quad (4)$$

The corresponding Doppler centre frequency is

$$f_{ac} = 2vR_0 \tan \theta / \lambda \sqrt{R_0^2 + R_0^2 \tan^2 \theta_i}. \quad (5)$$

Then by using the full-aperture imaging method in each subaperture, the subaperture SAR image can be achieved.

### B. SRC in subaperture

Along the range direction, do the Fourier transform, we can get

$$S(f_r, t_m) = \int_{-\infty}^{\infty} s(t, t_m) \exp(-j2\pi f_r t) dt \quad (6)$$

$$= A_0 A_1 \text{rect}\left(\frac{f_r}{B}\right) \text{rect}\left(\frac{t_m}{T_a}\right) \exp\left\{-j \frac{4\pi(f_r + f_0)R(t_m)}{c}\right\} \exp\left(-j \frac{\pi f_r^2}{k_r}\right).$$

Where  $f_r$  is range direction frequency,  $f_0$  is centre carrier frequency,  $k_r$  is range direction rate,  $k_r = B/T_p$ ,  $A_0$  and  $A_1$  are constant.

The range compression can be expressed as

$$S(f_r, t_m)' = S(f_r, t_m) H(f_r)$$

$$= A_0 A_1 \text{rect}\left(\frac{f_r}{B}\right) \text{rect}\left(\frac{t_m}{T_a}\right) \exp\left\{-j \frac{4\pi(f_r + f_0)R(t_m)}{c}\right\}. \quad (7)$$

Where  $H(f_r) = \exp(j\pi f_r^2/k_r)$  is the matched filter in range direction.

Along the azimuth direction, do the Fourier transform, we can get

$$S(f_r, f_a) = \int_{-\infty}^{\infty} S(f_r, t_m)' \exp(-j2\pi f_a t_m) dt_m \quad (8)$$

$$= A_0 A_1 A_2 \text{rect}\left(\frac{f_r}{B}\right) W_a(f_a - f_{ac}) \exp\left\{-j \frac{4\pi R_0 f_0}{c} \sqrt{D^2(f_a, v) + \frac{2f_r}{f_0} + \frac{f_r^2}{f_0^2}}\right\}.$$

Where  $D(f_a, v) = \sqrt{1 - c^2 f_a^2 / 4v^2 f_0^2}$ ,  $W_a(f_a - f_{ac})$  refers to the azimuth spectral envelope which centre is the Doppler centre frequency  $f_{ac}$ .

Then the secondary range compression can be expressed as

$$S(f_r, f_a)' = S(f_r, f_a) H_{src}(f_r, v)$$

$$= A_0 A_1 A_2 \text{rect}\left(\frac{f_r}{B}\right) W_a(f_a - f_{ac}) \exp\left\{-j \frac{4\pi R_0 f_0 D(f_a, v)}{c}\right\} \exp\left\{-j \frac{4\pi R_0 f_r}{c D(f_a, v)}\right\}. \quad (9)$$

Where  $H_{src}(f_r) = \exp(-j\pi f_r^2/K_{src})$  is the secondary range compression filter.

After the correction of range migration, the signal is

$$S(t, f_a) = S(f_r, f_a)' H_{RCMC}(f_r, f_a, v)$$

$$= A_0 A_1 A_2 B \sin c\left[B(t - \frac{2R_0}{c})\right] W_a(f_a - f_{ac}) \exp\left\{-j \frac{4\pi R_0 f_0 D(f_a, v)}{c}\right\}. \quad (10)$$

Where  $H_{RCMC}(f_r, f_a, v) = \exp\{j4\pi f_r R_0 (1 - D(f_a, v))/c D(f_a, v)\}$  is the range migration correction filter.

The azimuth compression can be expressed as

$$S(t, f_a)' = S(t, f_a) H(f_a)$$

$$= A_0 A_1 A_2 B \sin c\left[B(t - \frac{2R_0}{c})\right] W_a(f_a - f_{ac}). \quad (11)$$

Where  $H(f_a) = \exp\{j4\pi R_0 f_0 D(f_a, v)/c\}$  is the matched filter used in azimuth compression.

### C. Full-aperture imaging

When each subaperture has been azimuth focused, we only need to arrange all the subapertures in sequence, remove the overlapping data between the whole apertures, remove the displacement of each aperture reference point relative to zero Doppler frequency, and connect the centre frequency of different subaperture echos. Then we use IFFT in azimuth to get full-aperture image.

After frequency connection, the frequency width has contained all the band information. The whole process of connection can be regarded as a transformation process in the time domain. The final synthetic image in time domain can be expressed as

$$s(t, t_m) = \sum_{i=1}^I S_i(t, f_a)' \cdot e^{j2\pi f_{iac} t} \quad (12)$$

$$= A_0 A_1 A_2 B \sin c \left[ B \left( t - \frac{2R_0}{c} \right) \right] T_a \sin c(T_a t_m) \cdot$$

Where  $S_i(t, f_a)'$  is the  $i$ -th subaperture signal after SRC pulse compression in azimuth,  $f_{iac}$  is the range centre frequency of  $i$ -th subaperture. Now the signal has been compressed in the range and azimuth direction, range direction is compressed to  $2R_0/c$  and azimuth to  $t_m=0$ .

#### IV. ALGORITHM SIMULATION

According to the theory of Section III, we simulate the SSRC by point target imaging. The simulation parameters are shown in Table1, and this selection of parameters is based on the characteristics of the near space environment. Here we use two, four and eight subapertures under the squint angle of  $20^\circ$ , and compare with full-aperture SRC algorithm.

Table1. Simulation Parameters

Simulation Parameters	value
<i>Flight height</i>	50km
<i>Pulse width</i>	2.5 $\mu$ s
<i>Bandwidth</i>	50MHz
<i>Flight velocity</i>	100m/s
<i>Flight aperture length</i>	800m
<i>Azimuth beam width</i>	0.0125rad
<i>PRF</i>	100
<i>Carrier wave length</i>	0.05m
<i>Squint angle</i>	$20^\circ$

To estimate the effectiveness of the proposed SSRC algorithm, we simulate two-dimensional 8-point targets under the same conditions for near space squint SAR, respectively with SRC and SSRC for comparison. Fig.4 is the imaging results, where picture(a) is the full-aperture SRC algorithm, picture (b) is SSRC imaging result with 2 suba-

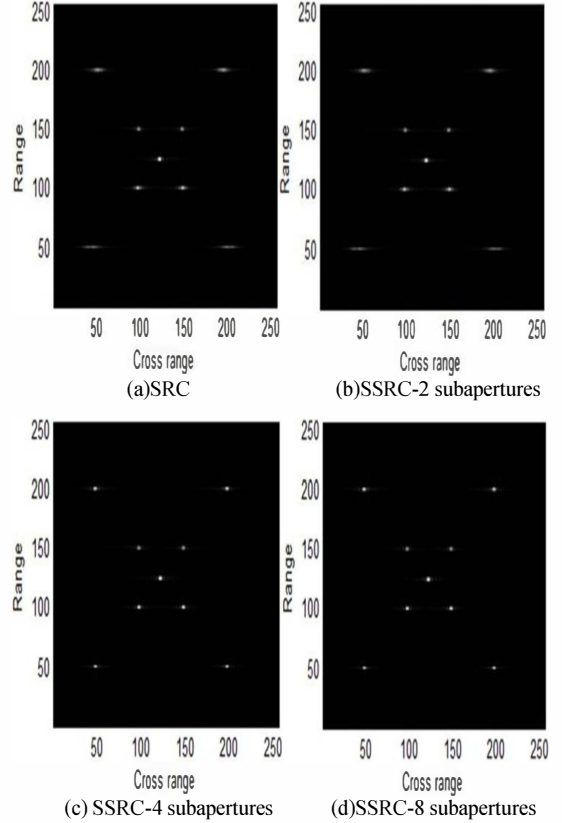


Fig.4. Imaging results

pertures, picture (c) is SSRC with 4 subapertures and picture (d) is SSRC with 8 subapertures.

Table2 gives the imaging performance index of two algorithms in azimuth, including the resolution (mainlobe -3 dB width), integral to side lobe ratio (ISLR), peak to side lobe ratio (PSLR) and total processing time for point target under different squint angles. We do not divide subaperture in the range direction, because the range direction algorithm is the same as full-aperture, so there is no obvious improvement of imaging results in range. We can see that the SSRC algorithm has clearer target points and better imaging quality than SRC under different squint angles and we can come to the conclusion that the improved SSRC algorithm is better.

Table 2. Simulation Results

Algorithms		SRC	SSRC (2 subapertures)	SSRC (4 subapertures)	SSRC (8 subapertures)
Squint angle 20°	Resolution (m)	0.59	0.53	0.51	0.5
	ISLR(dB)	-9.56	-9.73	-10.03	-10.19
	PSLR(dB)	-11.07	-11.34	-12.07	-12.43
	Single subaperture Time/Total Time (s)	17.15/17.15	8.93/18.05	4.55/18.76	2.66/19.78
Squint angle 40°	Resolution (m)	0.6	0.54	0.52	0.5
	ISLR(dB)	-8.78	-8.92	-9.07	-9.16
	PSLR(dB)	-10.01	-10.23	-10.69	-11.34
	Single subaperture Time/Total Time (s)	18.23/18.23	8.98/18.97	4.89/19.43	2.99/19.97
Squint angle 60°	Resolution (m)	0.76	0.71	0.68	0.61
	ISLR(dB)	-7.12	-7.43	-8.04	-8.53
	PSLR(dB)	-9.03	-9.38	-9.84	-10.23
	Single subaperture Time/Total Time (s)	19.05/19.05	9.54/19.53	5.65/19.83	3.87/20.21

## V. CONCLUSION

In this paper, SSRC algorithm is proposed for near space squint SAR imaging to solve the problems including the serious coupling between range and azimuth and overlong imaging synthetic aperture. The subaperture approach is introduced into the SRC algorithm, and the new imaging algorithm process is described in detail. Through the simulation and contrast with SRC, the advantages and application value of SSRC can be obviously shown and this improved algorithm is verified to be more effective in near space squint SAR imaging.

## ACKNOWLEDGMENT

This work is supported in part by NSFC 61143 008, National High Technology Research and Development Program of China (No. 2011AA01A204), the Fundamental Research Funds for the Central Universities.

## REFERENCES

- [1] L. C. Tomme, and C.S. Daul, "Balloons in Today's Military: An Introduction to the Near space Concept," *Air & Space Power Journal*, vol.19,no.4,pp.39-49, 2005.
- [2] W.Q. Wang, "Near space vehicles: Supply a gap between satellites and airplanes for remote sensing," *IEEE Trans. on AES*, vol.26,no.4,pp.4-9,2011.
- [3] M. Galletti, G. Krieger, B. Thomas, M. Marquart, and S. S. Johannes, "Concept Design of a Near space Radar for Tsunami Detection," *IEEE Trans. on Geosci. Remote Sens.*, vol.6, pp.34-37,2007.
- [4] G.W. Davidson, and I. Cumming, "Signal properties of space-borne squint-mode SAR," *IEEE Trans. on Geosci. Remote Sens.*, vol.35, no.3, pp.611-617,1997.
- [5] J.L. Walker, "Range Doppler Imaging of Rotating Object," *IEEE Trans. on AES*, vol.1, no.16, pp.37-43,1980.
- [6] C.Y. Chang, M. Jin, and J.C. Curlander, "Squint Mode SAR Processing Algorithms," *IGARSS*, vol.3, pp.1702-1706,1989.
- [7] W.Q. Wang, "Near space Wide-Swath Radar Imaging with Multiaperture Antenna," *IEEE Antennas and Wireless Propagation Letters*, vol.8, pp.461-464,2009.
- [8] Li Yueli, Yan Shaoshi, and Zhu Guofu, "Ultra wide band synthetic aperture radar real time processing with a subaperture nonlinear chirp scaling algorithm," *Synthetic Aperture Radar (APSAR)*, 2011 3rd International Asia-Pacific Conference on, pp.1-4, 2011.
- [9] J.C. Curlander, and R.N. McDonough, *Synthetic Aperture Radar: System and Signal*, Wiley, New York,1991.
- [10] T.s. Yeo, N.L. Tan, C.B. Zhang, and Y.H. Lu, "A new subaperture approach to high squint SAR processing," *IEEE Trans. on Geosci. Remote Sens.*, vol.39, no.5, pp.954-968, 2001.
- [11] Li Wei, "A New Improved Step Transform Algorithm for Highly Squint SAR Imaging," *Geoscience and Remote Sensing Letters*, *IEEE*, vol.8, no.1, pp.118-122, 2011.
- [12] Ping Zheng, Xiaojun Jing, Songlin Sun and Hai Huang, "Range Migration Subaperture Algorithm for Spotlight SAR in Near Space," *IEEE Network Infrastructure and Digital Content (IC-NIDC)*, Beijing, vol. 9, pp562-566, 2012.